

# Identification of Longitudinal Acoustic Modes Associated with Pressure Oscillations in Ramjets

W.H. Clark\*

Naval Weapons Center, China Lake, California  
and

J.W. Humphrey†

California Institute of Technology, Pasadena, California

A one-dimensional, isentropic analytical method is presented for calculating the longitudinal acoustic modes in an idealized "dump-type" ramjet engine. The analysis accounts for the complex acoustic admittances of the choked exit nozzle and of the normal shock in the supersonic inlet. The method assumes that all mean flow properties such as inlet and combustor temperatures, densities, and average Mach numbers are known. The predicted longitudinal modes are compared with data acquired from three different types of experiments. The first experiment concerned a wind tunnel model of a missile which utilized a ramjet with two side-dump inlets. The wind tunnel tests were primarily intended to determine the behavior of the supersonic inlets in the presence of downstream pressure oscillations. A mechanical device was used to excite periodic pressure perturbations in the simulated combustor exit. The second experiment involved connected pipe combustion tests of a side dump combustor. These tests included systematic changes in combustor length and in the entrance and exit boundary conditions. The third experiment utilized connected pipe tests of a coaxial dump combustor. The geometric length of the combustor was varied in order to examine the effects on combustion instability.

## Nomenclature

$A$	= inlet or combustor cross-sectional area
$\hat{A}$	= complex acoustic admittance function
$a_n$	= mean sound speed
$K_n$	$= (\omega_j + i\alpha_j)/a_n (1 - M_n^2)$
$L_1$	= effective inlet length
$L_2$	= effective combustor length
$M$	= mean Mach number
$M_{1S}$	= supersonic Mach number ahead of normal shock
$M_{2S}$	= Mach number behind normal shock
$p'_n(x, t)$	= fluctuating part of pressure
$P_n^+, P_n^-$	= amplitudes of right and left running acoustic waves
$P_T$	= inlet or combustor total pressure
$S$	= cross-sectional area of inlet diffuser
$T_{T0}$	= total temperature of inlet air
$T_{T4}$	= total temperature of combustor gases at entrance to exit nozzle
$U'_n$	= fluctuating part of velocity
$W_a$	= engine mass flow rate
$x$	= longitudinal position in the engine location
$x_{SH}$	= location of normal shock in inlet
$\alpha_j$	= damping part of $j$ th longitudinal mode
$\beta$	= complex acoustic reflectance
$\gamma_n$	= specific heat ratio
$\phi(x)$	= relative phase of acoustic pressure mode
$\Delta p(x)$	= pressure mode shape function
$\phi$	= fuel-to-air equivalence ratio
$\omega_j$	= frequency part of $j$ th longitudinal mode

## Subscripts

1 or 1.5	= inlet section
2 or 3	= combustor section
4	= combustor location at entrance to exit nozzle
5	= exit nozzle throat location
$n = 1, 2$	= denotes inlet or combustor section
$E$	= exit nozzle
$I$	= inlet section

## Introduction

THIS paper is a continuation and an expansion of two previous papers<sup>1,2</sup> dealing with the subject of combustion instabilities in modern integral rocket ramjets. The two previous papers provided tentative identification of longitudinal acoustic modes associated with combustion-induced pressure oscillations in both a full-scale side dump engine<sup>1</sup> and a laboratory-scale simulation of the same engine.<sup>2</sup> In the current paper, a relatively simple, idealistic analytical method is outlined for predicting the longitudinal acoustic modes that may occur in a ramjet engine. The predictions are then compared with the above-mentioned laboratory-scale engine. In addition, comparisons are made between predicted and measured longitudinal modes in a small wind tunnel model of a side dump engine and for a laboratory-scale coaxial dump engine. In general, predicted and experimental modes are in reasonable agreement for all three engines (or models) despite the simplifications of the analytical method.

There is, however, no attempt made to predict the *actual* stability characteristics of an engine. Rather, the naturally occurring longitudinal acoustic modes that *may* be present are calculated, and experimental evidence is used to determine if any of these modes are excited during unsteady combustion. Some stability studies have been done which deal with different mechanisms. Reardon studied the stability of ramjet oscillations of very low frequency that were lower than any of the longitudinal modes of the combustor alone.<sup>3</sup> Abouseif et al. studied the stability of oscillations driven by incomplete combustion.<sup>4</sup> The present experiments had sufficiently long combustors to have complete combustion.

Presented as Paper 84-1405 at the AIAA/SAE/ASME 20th Joint Propulsion Conference, Cincinnati, OH, June 11-13, 1984; received Sept. 4, 1984; submitted Dec. 1985. This paper is declared a work of the U.S. Government and is not subject to copyright protection in the United States.

\*Aerospace Engineer. Member AIAA.

†Graduate Student. Member AIAA.

Success in predicting many of the features of the excited mode which actually occur in complex, three-dimensional, chemically reacting flows gives confidence that future, more complete analyses will eventually result in useful design tools for predicting stability of a specific configuration. In order to provide useful experimental data for such future analyses, the present paper will present additional details on previously unpublished test results.

### Acoustic Model

The analytical model used is actually a simplified version of the technique described by Yang and Culick.<sup>5</sup> The current model does not include the approximate treatment of the two-dimensional features of the mean flowfield in the combustor, as was done by Yang and Culick.<sup>5</sup> This model is a strictly one-dimensional treatment of the configuration depicted in Fig. 1. The idealized ramjet model consists of an inlet section with known uniform mean flow properties connected via a sudden expansion to a combustion chamber with different, but uniform, mean flow properties. This allows for the greatly differing temperatures and sonic velocities that would typically occur between the inlet duct and the combustion chamber. The entrance to the inlet and the exit from the combustor are characterized by complex reflection coefficients which will be described later.

The appropriate solutions to the linearized conservation equations for the perturbation pressure  $p'_n$  and velocity  $U'_n$ , are

$$p'_n = (P_n^+ e^{iK_n x} + P_n^- e^{-iK_n x}) e^{-iM_n K_n x} \quad (1a)$$

and

$$U'_n = \frac{1}{\rho_n a_n} (P_n^+ e^{iK_n x} - P_n^- e^{-iK_n x}) e^{-iM_n K_n x} \quad (1b)$$

where the subscript  $n$  is  $n=1$  for the inlet section and  $n=2$  for the combustor section and  $P_n^+$  and  $P_n^-$  represent the amplitudes of right (+) and left (-) running acoustic waves. The time dependence in Eqs. (1a) and (1b) has been omitted but is assumed to be sinusoidal.

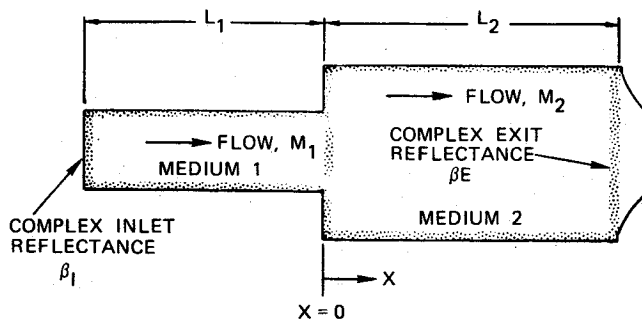


Fig. 1 Model of ramjet.

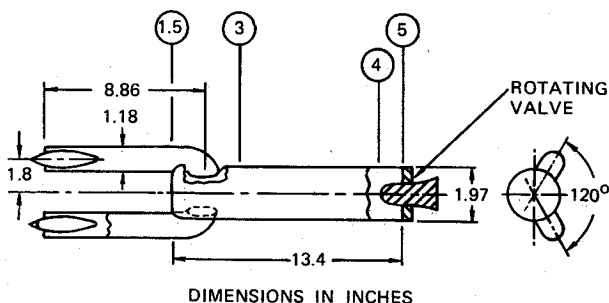


Fig. 2 Dimensions of side dump wind tunnel model.

At the dump plane ( $x=0$ ), the conditions of pressure and mass continuity result in

$$p'_1 = p'_2 \quad (2a)$$

$$\rho_1 A_1 U'_1 = \rho_2 A_2 U'_2 \quad (2b)$$

To obtain the mass continuity relation, Eq. (2b), it is important to use the isentropic flow assumption. The exit from the combustor ( $x=L_2$ ) is a choked nozzle with an axial length generally much shorter than the highest acoustic wavelength of interest. The acoustic admittance given by  $A = \rho a U' / p'$  at  $x=L_2$  is used to determine the complex reflectance  $\beta_E$  at the exit where  $\beta_E = (1 - \hat{A}_E) / (1 + \hat{A}_E)$  and  $\hat{A}_E = (\gamma_2 - 1)(M_2)/2$ . The quantity is the reflection coefficient which is, effectively, the ratio of reflected to incident pressure amplitudes.

The inlet entrance is treated in a similar manner, where  $\beta_I = (1 - \hat{A}_I) / (1 + \hat{A}_I)$ . The inlet admittance is more complicated than for the exit nozzle and is a function of the particular type of experimental setup. For instance, in some connected pipe tests the inlet can be approximated by an ideal open end with  $\beta_I = -1.0$ . For an actual ramjet or for a freejet test, however, a supersonic inlet operating under supercritical conditions is typical. In this case the reflection coefficient is determined by the interactions between upstream moving acoustic waves and the terminal normal shock system in the inlet diffuser. The inlet admittance function can then be calculated from the theory of Culick and Rogers.<sup>6</sup>

The mass and pressure continuity relations [Eqs. (2a) and (2b)] and the end conditions are used with Eqs. (1a) and (1b) to derive a transcendental equation for the unknown complex frequency:

$$(\beta_I \cdot F1 + 1)(1 - \beta_E \cdot F2) [(a_1 A_2) / (a_2 A_1)] = (\beta_I \cdot F1 - 1)(1 + \beta_E \cdot F2) \quad (3)$$

where

$$F1 = (e^{2K_1 L_1}) \quad \text{and} \quad F2 = (e^{2K_2 L_2})$$

The only unknown in Eq. (3) is the complex frequency.

After the complex frequency is known, the corresponding perturbation pressure mode shape can be computed for each frequency [from Eq. (1a)] for both the inlet and combustor as a function of  $x$ . Humphrey has published a more complete description of the theoretical method as well as a listing of the numerical method for solving Eq. (3) and computing the mode and phase distribution.<sup>7</sup>

The analytical acoustic model described in this paper contains no mechanisms for adding fluctuating energy to the flow. It does, however, include the steady state jump in energy level at the dump plane. Furthermore, the theory of Culick and Rogers<sup>6</sup> predicts that, in general, the normal shock at the inlet will tend to absorb acoustic energy, ( $|\beta_I| < 1.0$ ). Hence, all solutions obtained with the present model are stable ( $\alpha_j < 0$ ), as shown later in Fig. 3.

Table 1 The conditions for side dump wind tunnel model

$M_\infty$	= 2.8
$T_{70}$	= 504°R
$T_{74}$	= 504°R
$M_{1.5}$	= 0.25
$M_4$	= 0.18
$P_{71.5}$	= 30 psia
$M_{15}$	= 1.8
$x_{sh}^a$	= 1.7 in.
$A_3/A_{1.5}$	= 1.39
$A_4/A_5$	= 3.2

<sup>a</sup> $x_{sh} = 0$  (inlet cowl lip).

## Experimental Data

### Wind Tunnel Model

Figure 2 presents a sketch of a wind tunnel model of a missile which uses a two-inlet, side dump ramjet engine. The primary purpose of the tests with the model was to establish the behavior of the inlets under conditions of combustor pressure oscillations. In order to simulate the effects of combustion-induced pressure oscillations, a mechanical device was designed which would produce oscillatory pressures at the exit end of the combustor section. This device consisted of a translating valve which could be used to slowly vary the primary exit area; hence, a mean combustor pressure was

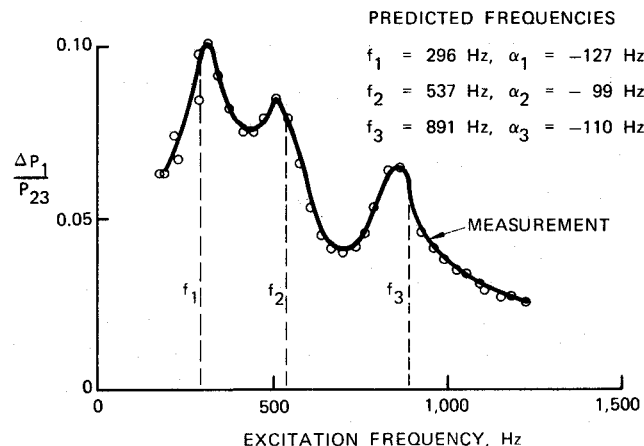


Fig. 3 Normalized inlet pressure oscillations as a function of excitation frequency.

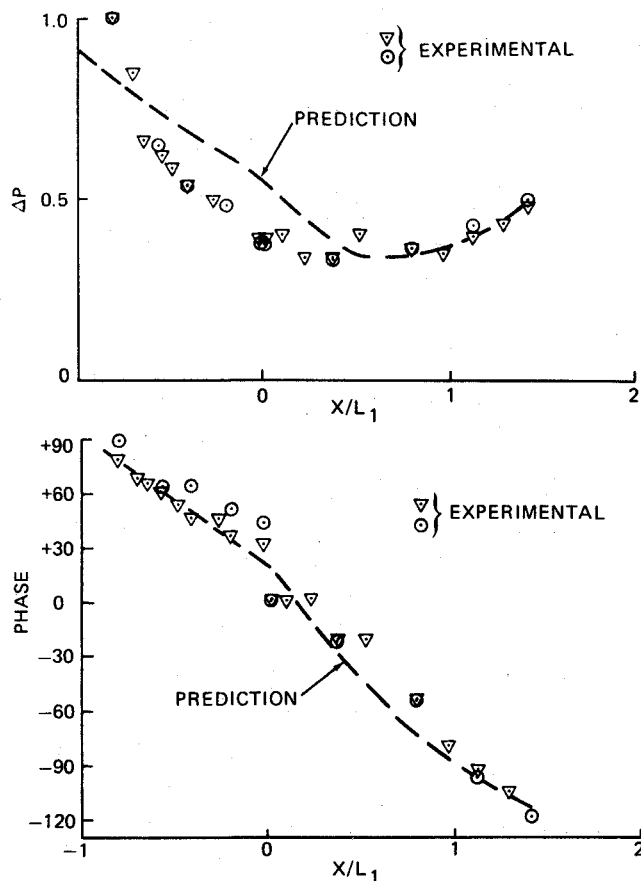


Fig. 4 Relative pressure amplitude and phase distributions for 310 Hz excitation frequency ( $p \times 3.1 = p$ , psi). (Phase is referenced to dome static pressure.)

established. Perturbations upon this mean pressure were produced by a rotating hole plate which produced a periodic secondary exit area and a corresponding rapidly varying exit pressure.

Typical test conditions are given in Table 1. The location of the steady-state terminal normal shock (which is required for the inlet boundary condition) is approximate and is based on the ideal one-dimensional isentropic and normal shock relations, the known area distribution, and the requirement that  $M_{1.5} = 0.25$ . The predictions for the side dump combustors were done with the crude approximation that the total inlet area (the sum of the two side inlets) to combustor area be used in the model. This certainly introduces some of the errors found in the inlet predictions.

During tests the hole plate was rotated at varying speeds and the resulting oscillating pressures were measured by means of high-frequency pressure transducers distributed longitudinally along the inlet/combustor configuration. Figure 3 shows the oscillating pressure amplitude measured in the inlet. The resonant frequencies at 310, 550, and 850 Hz are in good agreement with the predicted values as indicated on the figure.

The measured root-mean-square pressure oscillations and relative phase distributions for the 310 Hz excitation frequency are shown on Fig. 4 along with the predicted values. The relative phase distributions are in fair agreement for both excitation frequencies of 310 Hz (shown) and 550 Hz (not shown). The pressure mode shape predictions are qualitatively correct, although the agreement in magnitude is poor, especially for the 550-Hz mode.

### Side Dump Combustor

The laboratory scale, side dump engine depicted in Fig. 5 has been previously described.<sup>2</sup> Briefly, this engine was tested in a direct connect mode with both inlets connected to a large plenum via the converging-diverging nozzles shown. Liquid fuel (RJ-4) was introduced into the inlet air flows through fixed-orifice injectors which have been described.<sup>1</sup> The pressure oscillations were measured with the high-frequency pressure transducers located as shown on Fig. 5. Systematic variations about this "baseline" configuration were made in order to evaluate the acoustic mode predictions. In addition to the "baseline" (Configuration I), three other configurations were tested. In each case, only one geometric parameter was varied. Briefly, in Configuration II, the combustor exit nozzle area was increased in order to reduce the combustor pressure and increase the average combustor Mach number. In this case, a sharp-edged orifice plate was used at the combustor exit rather than a contoured nozzle. In Configuration III, the combustor length was decreased in order to shift the frequencies of acoustic modes. In Configuration IV, the inlet nozzles were replaced with straight pipe sections in order to simulate an acoustically open end. The pertinent test conditions for each configuration are given in Table 2.

The tests with the converging-diverging inlet nozzles (Configurations I, II, and III) indicated that the nozzles were

Table 2 Test conditions for side dump combustor

Test no.	1	2	3	4
Configuration	I	II	III	IV
$T_{70}$ , °R	1010	1061	1135	1065
$T_{74}$ , °R	4150	3680	3234	3800
$M_{1.5}$	0.23	0.27	0.28	0.26
$M_{1S}$	1.01	1.01	1.1	NA
$M_4$	0.37	0.524	0.37	0.44
$P_{74}$ , psia	88	63	56	75
$\phi^a$	0.91	0.93	<sup>b</sup>	0.91
$x_{SH}$ , in.	≈ 0.25	0.25	0.25	NA
$\dot{W}_a$ , lb/s	5	5	3.6	5.1

<sup>a</sup>RJ-4 fuel was used with stoichiometric fuel/air ratio = 0.07. <sup>b</sup>C<sub>2</sub>H<sub>4</sub> fuel was used with unknown fuel flow rate.

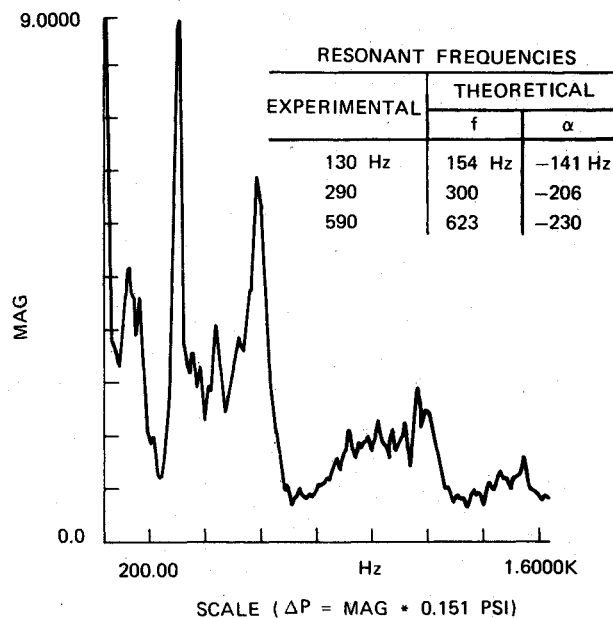
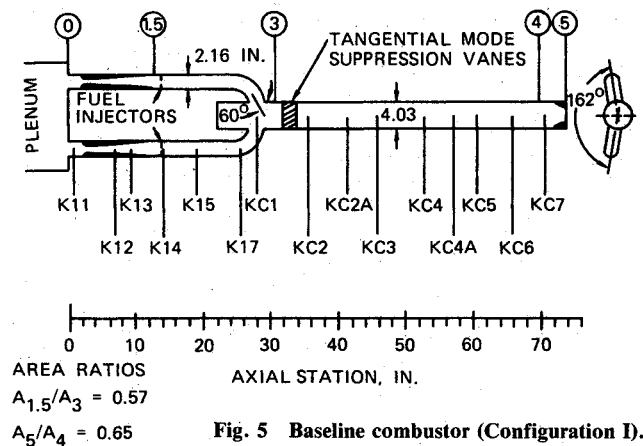


Fig. 6 Amplitude spectrum at KC4 for Configuration I.

Table 3 Test conditions for coaxial dump engine

Test no.	D121	D114	D164	D163
Configuration	1	1	3	2
$L_1$ , in.	38.5	38.5	38.5	38.5
$L_2$ , in.	30.1	30.1	15.1	22.6
$T_{70}$ , °R	860	860	860	860
$T_{74}$ , °R	3000	3000	3000	4000
$M_{1S}$	1.8	1.8	1.8	1.8
$M_{2S}$	0.62	0.62	0.62	0.62
$x_{SH}$ , in.	1.6	1.6	1.6	1.6
$M_4$	0.21	0.21	0.21	0.21

Test no.	Configuration	Predicted frequency		Experimental frequency
		f	$\alpha$	
D121, D114	1	118	-50	175
		303	-60	540
		535	-50	
D164	3	138	-54	300
		303	-65	
		482	-73	
		665	-77	
D163	2	134	-52	190
		296	-63	
		469	-68	
		735	-65	650
		770	-59	

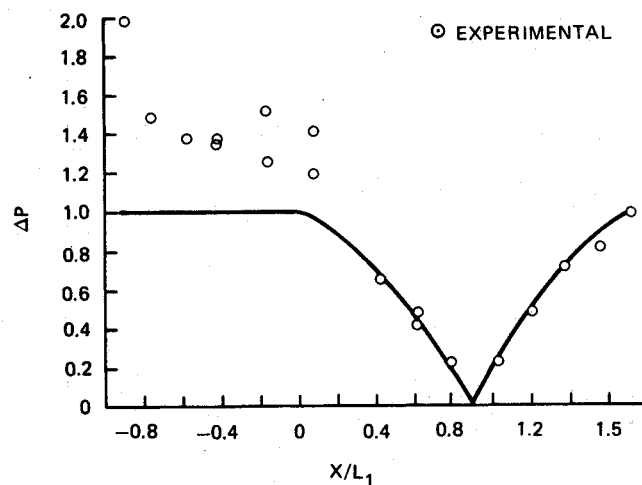


Fig. 7 Pressure amplitude at 290 Hz for Configuration I.

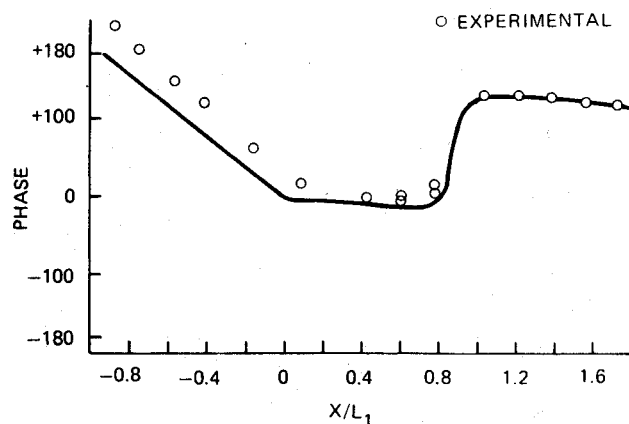


Fig. 8 Relative phase distribution at 290 Hz for Configuration I.

periodically unchoked during combustion. Hence, the application of the theory of Culick and Rogers<sup>6</sup> is not strictly correct for the inlet boundary conditions. Nevertheless, reasonable results were obtained by estimating the average Mach number upstream of the shock ( $M_{1S}$ ) to be the values shown in Table 2.

Results from Test 1 are indicated in Fig. 6, which shows the pressure amplitude spectrum obtained by digital spectral analysis of the signal from one of the high-frequency transducers. The oscillations are dominated by the mode at 290 Hz, but there are also significant spectral components at 130 and 590 Hz. The agreement between experimental and theoretical frequencies is very good, as indicated. The solution to Eq. (3) for the conditions of Tests 1, 2, and 3 indicated that all the natural acoustic modes are highly damped. This is because the inlet reflection coefficient  $\beta_I$  is approximately  $\beta_I = 0$  for the nearly sonic conditions listed in Table 2. In order to obtain reasonable comparisons with experimental mode shapes and phase distributions, it was necessary to set  $\alpha_I = 0$ . This is physically reasonable since the simple theoretical model contains no mechanism to replace the acoustic energy lost at the anechoic inlet end ( $\beta_I = 0$ ), although experimentally the oscillations are being driven at a constant amplitude by the combustion heat addition.

The pressure amplitude mode shapes and relative phase distribution for experimental and theoretical values are compared in Figs. 7 and 8 for the 290 Hz mode. The agreement between theory and experiment for pressure amplitudes is good in the combustor and poor in the inlet sections. The relative phase distributions agree well throughout the engine. This is also true for the 130 and 590 Hz modes (not shown). It

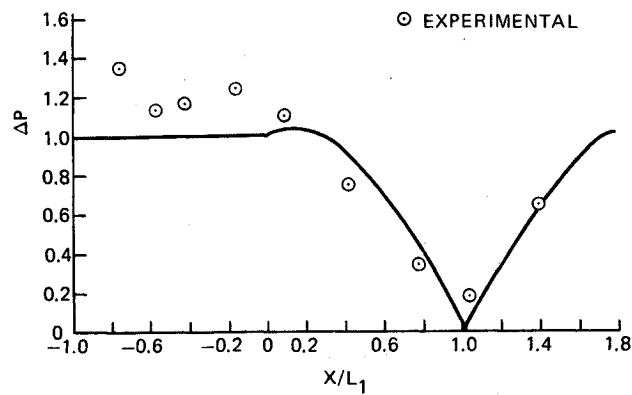


Fig. 9 Pressure amplitude at 255 Hz for Configuration II ( $p \times 14 = p$ , psi).

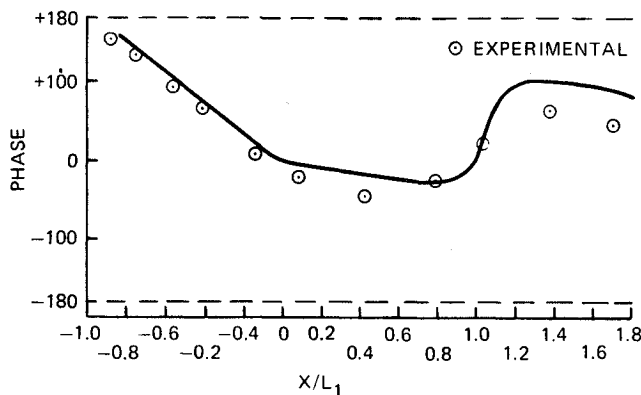


Fig. 10 Relative phase distribution at 255 Hz for Configuration II.

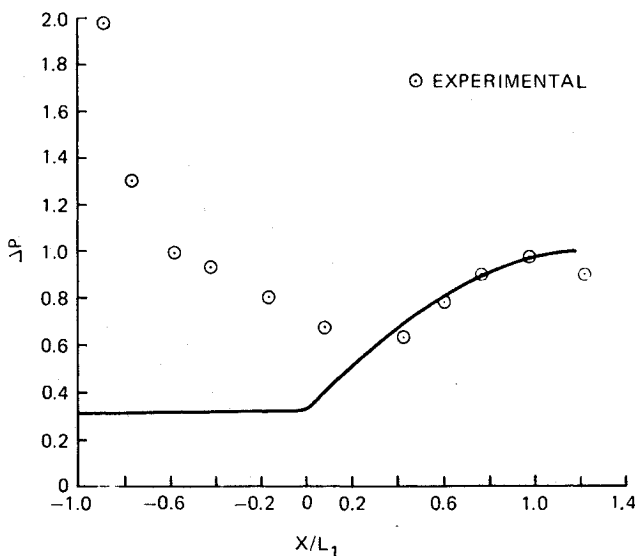


Fig. 11 Pressure amplitude at 233 Hz for Configuration III ( $p \times 4.86 = p$ , psi).

is interesting to notice that the mode at 130 Hz, which has been called a "bulk" mode,<sup>1,2</sup> has a corresponding predicted mode. The term "bulk" mode has been used to denote the low frequency mode with a relatively constant phase distribution. It should be noted that these "bulk" modes are not independent of the acoustics of the system.<sup>8</sup>

Test 2 (Configuration II) was not significantly different from Test 1 and the agreement between theory and experiment was about the same as for Test 1 (Figs. 9 and 10). The experimental frequencies were 150, 255, and 500 Hz while the predicted frequencies were 129, 272, and 566 Hz.

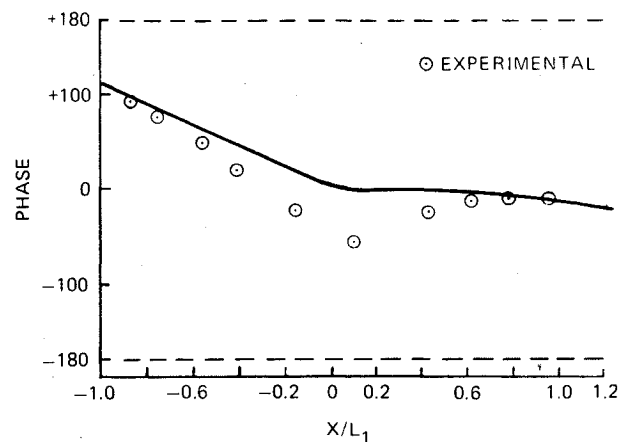


Fig. 12 Relative phase distribution at 233 Hz for Configuration III.

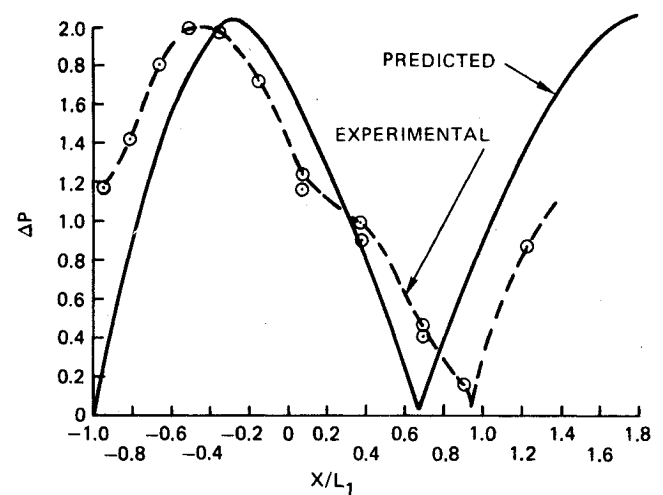


Fig. 13 Pressure amplitude at 290 Hz for Configuration IV.

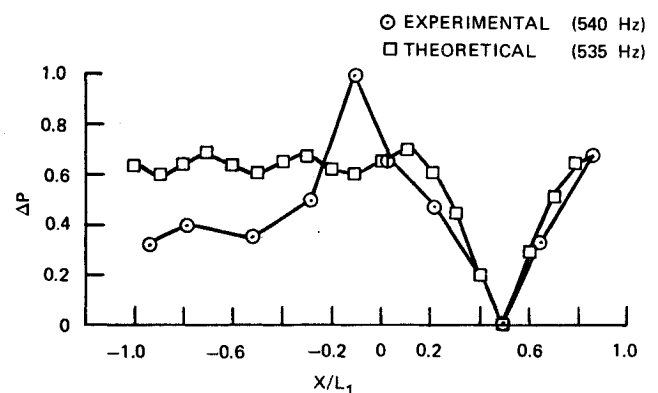


Fig. 14 Pressure mode shape for coaxial dump ramjet, Configuration 1, Test D121.

For Test 3 (Configuration III) with the short combustor, the dominant oscillatory mode was at 223 Hz. The mode and phase plots of Figs. 11 and 12 reveal that this was the same as the "bulk" mode which was present during Tests 1 and 2 for the longer combustor. In Configuration III, however, the frequency of the dominant mode was not in good agreement with the predicted value, nor was the pressure mode shape in the inlet region. The relative phase distributions (Fig. 12) were in relative agreement. The experimental frequencies were 223, 373, and 450 Hz while the predicted frequencies were 170, 361, and 532 Hz.

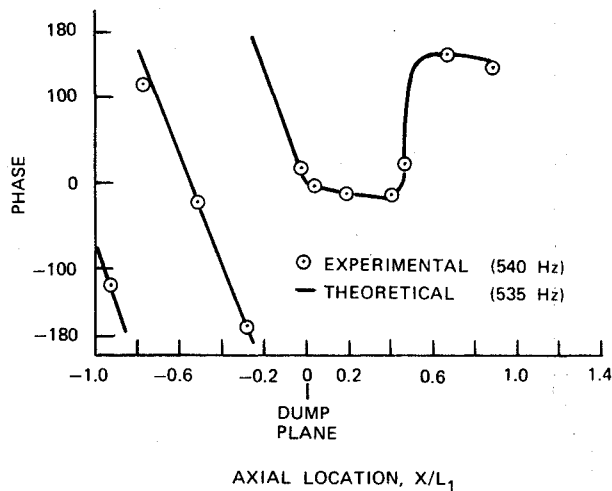


Fig. 15 Relative phase distribution for coaxial dump ramjet, Configuration 1, Test D121.

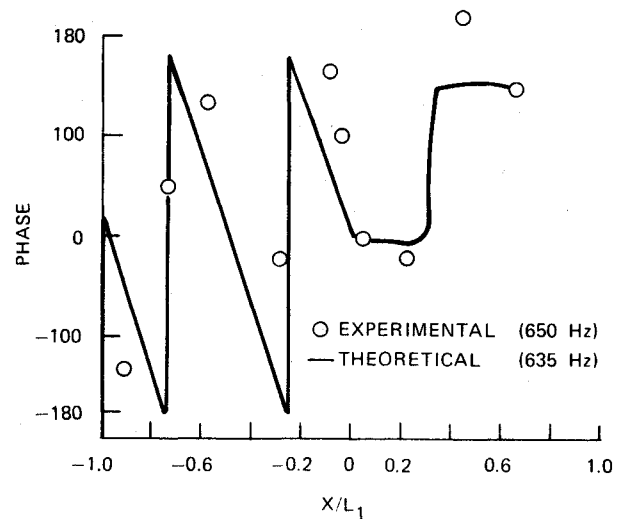


Fig. 17 Relative phase distribution for coaxial dump ramjet, Configuration 2, Test D163.

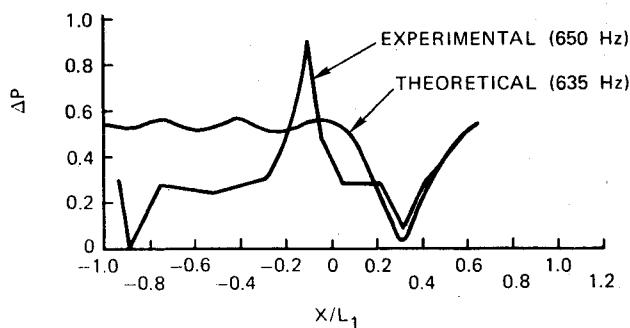


Fig. 16 Pressure mode shape for coaxial dump ramjet, Configuration 2, Test D163.

For Test 4 the dominant mode was at 292 Hz. For Configuration IV with an "open" inlet as the upstream boundary condition, the inlet reflection coefficient was ideally  $\beta_I = -1.0$ . The pressure mode shape shown in Fig. 13 indicates that this change in end conditions did, indeed, have a profound influence on the mode shapes in the inlet section. However, the results in this case indicate a considerable discrepancy between experiment and the analysis. Further study of the boundary condition  $\beta_I$  showed that the plenum chamber could no longer be ignored. When the plenum was considered in a similar acoustic analysis, the predictions were similar to those of Tests 1 and 3.

### Coaxial Dump Combustor

A coaxial dump, research-scale combustor has been previously described.<sup>9-11</sup> Briefly, this combustor uses a rectangular choked inlet diffuser, an inlet duct, a coaxial dump plane and combustor terminated by a choked nozzle. Either gaseous  $C_2H_4$  fuel or liquid (JP-4) fuel or combinations of the two were used. Configuration 1 of Table 3 exhibited two modes of oscillation at 175 and 540 Hz. The corresponding predicted acoustic frequencies are 118 and 535 Hz. The comparisons between pressure modes and relative amplitudes for the 535 Hz mode are given in Figs. 14 and 15. Similar results for the 118 Hz mode exists. The experimental pressure modes were taken from the maximum values of the pressure oscillation envelopes given elsewhere.<sup>9</sup> As in the dump combustor, the agreement between experimental and theoretical phases is satisfactory, whereas the pressure mode shapes agree only in the combustor section but not in the inlet. Configuration 3 with a short combustor exhibited a dominant instability at 300 Hz which agrees almost exactly with one of the predicted

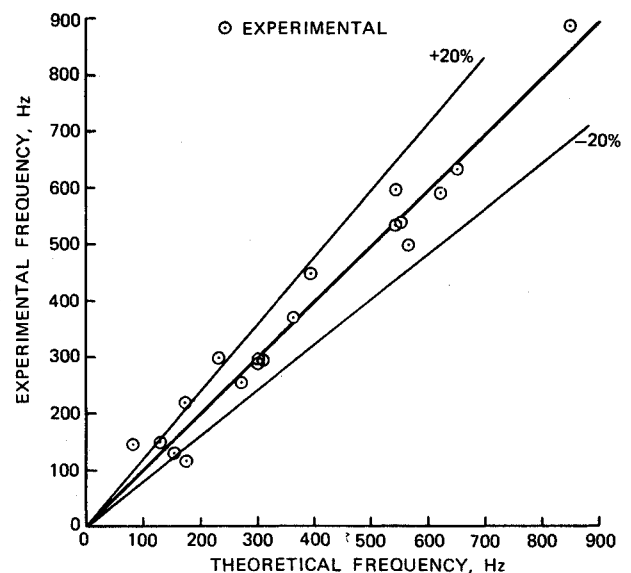


Fig. 14 Comparison of experimental and theoretical frequencies for all cases discussed in this paper.

acoustic modes for this configuration, as given in Table 3. However, the agreement between predicted and experimental pressure mode shapes is poor while the relative phase distributions are in reasonable agreement.

Finally, Configuration 2 exhibited modes at 190 and 650 Hz, as indicated in Table 3. The 190 Hz mode is the same as the 175 Hz mode observed for Configuration 1 in Test D114.<sup>9</sup> The amplitude and relative phase plots for the 650-Hz mode are shown in Figs. 16 and 17. As in previous examples, the pressure amplitudes in the combustor agree well with the predicted acoustic mode, and the relative phases are in qualitative agreement.

### Summary and Conclusion

From the preceding discussions, it is clear that a simple, one-dimensional, isentropic theory for the acoustic modes of an idealized ramjet engine is capable of correctly predicting many of the features of pressure oscillations which are known to occur in actual practice. In general, the agreement between theoretical and measured phase distributions and between theoretical and measured pressure amplitude mode shapes in the combustor region is satisfactory. However, in the inlet sec-

tions of both the side dump and coaxial dump engines, there was considerable discrepancy between measured and theoretical pressure mode shapes. A summary of experimental vs measured frequencies for all tests discussed in this paper is given in Fig. 18. With a few exceptions, the agreement is within  $\pm 20\%$  for the wide range of configurations and test conditions examined.

The modes excited for the small wind tunnel model with mechanical excitation differed considerably from those observed in the combustion tests of the side and coaxial dump engines. The theoretical *damped* solutions were in reasonable agreement with experiment. The phase distributions indicate that pressure disturbances generated at the exit end of the model propagate upstream and are absorbed at the inlet shock structure. There is no experimental evidence that pressure nodes exist in the simulated combustor section, although this would be expected if strong reflections and cancellations of acoustic waves occurred.

The side dump and coaxial dump engines each exhibited two types of oscillations. The first type is identified by the presence of one or more pressure node points in the combustor sections. (For example, see Figs. 7, 9, 13, 14, and 16.) Each pressure node point is associated with a rapid (approximately 180 deg) phase shift, as demonstrated in Figs. 8, 10, 15, and 17. The other common mode is identified by comparatively uniform values of the pressure oscillation amplitude and relative phase throughout the combustor section. With one exception, in the inlet section of *all* the configurations considered, the relative phase distribution varied linearly with longitudinal position and with a slope in fair agreement with the theoretical value. Theoretically, this linear variation is due to the fact that for the upstream normal shock reflection coefficient  $|\beta_I| \ll 1.0$ . Hence, the inlet entrance does not strongly reflect the upstream moving waves. The exceptional condition is for Configuration IV of the side dump combustor series. For this case, the upstream end should have approximated an ideal open acoustic end for which  $\beta_I = -1.0$ . The predicted and experimental pressure mode shapes in the inlet section were in qualitative agreement while the slopes of the phase variations differed considerably. Surprisingly, the measured

results show that the same linear phase variation occurred in this open-ended inlet as in the nearly choked inlet.

## References

- <sup>1</sup>Clark, W.H., "Experimental Investigation of Pressure Oscillations in a Side Dump Ramjet Combustor," *Journal of Spacecraft and Rockets*, Vol. 19, Jan.-Feb. 1982, pp. 47-53.
- <sup>2</sup>Clark, W.H., "Geometric Scale Effects on Combustion Instabilities in a Side Dump Liquid Fuel Ramjet," *Proceedings of the 19th JANNAF Combustion Meeting*, CPIA Pub. 366, Vol. 1, Oct. 1982, pp. 595-604.
- <sup>3</sup>Reardon, F.H., "Analysis of Very Low Frequency Oscillations in a Ramjet Combustor by Use of a Sensitive Time Lag Model," *Proceedings of the 18th JANNAF Combustion Meeting*, Pasadena, CA, CPIA Pub. 347, Vol. 3, Oct. 1981, pp. 307-316.
- <sup>4</sup>Abouseif, G.E., Keklak, J.A., and Toong, T.Y., "Ramjet Rumble: The Low-Frequency Instability Mechanisms in Coaxial Dump Combustors," *Combustion Science and Technology*, Vol. 36, March 1984, pp. 83-108.
- <sup>5</sup>Yang, V. and Culick, F.E.C., "Linear Theory of Pressure Oscillations in Liquid Fueled Ramjet Engines," AIAA Paper 83-0574, Jan. 1983.
- <sup>6</sup>Culick, F.E.C. and Rogers, T., "The Response of Normal Shocks in Diffusers," *AIAA Journal*, Vol. 21, Oct. 1983, pp. 1382-1390.
- <sup>7</sup>Humphrey, J.W., "Combustion of One-Dimensional Acoustic Modes as Applied to Ramjet Inlet/Combustors," Naval Weapons Center, China Lake, CA, NWC TM 5164, 1983.
- <sup>8</sup>Culick, F.E.C., "Some Nonacoustic Instabilities in Rocket Chambers are Acoustic," *AIAA Journal*, Vol. 6, July 1968, pp. 1421-1423.
- <sup>9</sup>Crump, J.E., Schadow, K.C., Blomshield, F.S., Culick, F.E.C., and Yang, V., "Combustion Instability in Dump Combustors: Acoustic Mode Determinations," *Proceedings of the 19th JANNAF Combustion Meeting*, CPIA Pub. 366, Vol. 1, Oct. 1982, pp. 307-316.
- <sup>10</sup>Schadow, K.C., Crump, J.E., and Blomshield, F., "Combustion Instability in a Research Dump Combustor: Inlet Shock Oscillations," *Proceedings of the 18th JANNAF Combustion Meeting*, Pasadena, CA, CPIA Pub. 347, Vol. 3, Oct. 1981, pp. 341-356.
- <sup>11</sup>Crump, J.E., Schadow, K.C., Blomshield, F., and Bicker, C.J., "Combustion Instability in a Research Dump Combustor: Pressure Oscillations," *Proceedings of the 18th JANNAF Combustion Meeting*, Pasadena, CA, CPIA Pub. 347, Vol. 3, Oct. 1981, pp. 357-370.